

Experimental study of particle transport and density fluctuation in LHD

K.Tanaka¹⁾, S. Morita¹⁾, A. Sanin¹⁾, L.N. Vyacheslavov¹⁾, C. Michael¹⁾, K.Kawahata¹⁾, S. Murakami³⁾, A. Wakasa⁴⁾, H. Yamada¹⁾, J. Miyazawa¹⁾, T. Tokuzawa¹⁾, T.Akiyama¹⁾, M.Goto¹⁾, K. Ida¹⁾, M. Yoshinuma¹⁾, K. Narihara¹⁾, I.Yamada¹⁾, M. Yokoyama¹⁾, S. Masuzaki¹⁾, T. Morisaki¹⁾, R.Sakamoto¹⁾, H.Funaba¹⁾, A.Komori¹⁾ and LHD experimental group

1)National Institute for Fusion Science, 322-6 Oroshi, Toki, 509-5292, Japan

2)Budker Institute of Nuclear Physics, 630090, Novosibirsk, Russia

3)Department of Nuclear Engineering, Kyoto University, Kyoto 606-8501, Japan

4)Graduate School of Engineering, Hokkaido University, Sapporo, 060-8628, Japan

e-mail contact of main author: ktanaka@LHD.nifs.ac.jp

Abstract. A variety of electron density (n_e) profiles have been observed in Large Helical Device (LHD). The density profiles change dramatically with heating power and toroidal magnetic field (B_t) under the same line averaged density. The particle transport coefficients, i.e., diffusion coefficient (D) and convection velocity (V) are experimentally obtained from density modulation experiments in the standard configuration. The values of D and V are estimated separately at the core and edge. The diffusion coefficients are strong function of electron temperature (T_e) and are proportional to $T_e^{1.7 \pm 0.9}$ in core and $T_e^{1.1 \pm 0.14}$ in edge. And edge diffusion coefficients are proportional to $B_t^{-2.08}$. It is found that the scaling of D in edge is close to gyro-Bohm-like in nature. The existence of non-zero V is observed. It is observed that the electron temperature (T_e) gradient can drive particle convection. This is particularly clear in the core region. The convection velocity in the core region reverses direction from inward to outward as the T_e gradient increases. In the edge, the convection is inward directed in the most of the case of the present data set. And it shows modest tendency, whose value is proportional to T_e gradient keeping inward direction. However, the toroidal magnetic field also significantly affects value and direction of V . The spectrum of density fluctuation changes at different heating power suggesting that it has an influence on particle transport. The peak wavenumber is around 0.1 times the inversed ion Larmor radius, as is expected from gyro-Bohm diffusion. The peaks of fluctuation intensity are localized at the plasma edge, where density gradient becomes negative and diffusion contributes most to the particle flux. These results suggest a qualitative correlation of fluctuations with particle diffusion.

1. Introduction

Particle transport of bulk ions and electrons is one of the most important issues of magnetically confined plasma research. However, compared with energy transport study, fewer works have been done. This is because of the difficulties of the experimental estimation of the particle source and the existence of the convection term in the particle balance equation. These make estimation of particle transport coefficients, i.e., diffusion coefficients (D) and convection velocity (V) impossible from simple particle balance analysis in the equilibrium state. Large Helical Device (LHD) is a large heliotron whose operational envelope extends towards the fusion relevant regime. Although thermal transport has been discussed in many reports, this is the first systematic study of the bulk ion and electron particle transport in LHD. The diffusion coefficients and convection velocities are separately estimated from the propagation of periodically modulated density by controlling the gas puff.

In most of the operational regimes of LHD, particle transports is dominated by anomalous transport. Therefore, experimental study of the turbulence is also important. In this paper, characteristic of the electron density fluctuation, which can play role on particle confinements are also described.

2. Density profiles in LHD

The density profiles in LHD change with the magnetic configuration, magnetic field strength, and heating power. This is because the characteristics of particle transport are determined by these experimental conditions. Figure 1 show T_e and n_e profiles at different neutral beam injection (NBI) heating power. The magnetic configuration is the so-called standard configuration, whose magnetic axis position (R_{ax}) is 3.6m. This configuration has the largest plasma volume and achieves the highest stored energy and best energy confinement improvement [4].

As shown in Fig.1 (a), T_e increases with increasing heating power. The shape of the T_e profiles remains parabolic and peaked at the center almost regardless of the heating power. On the other hand, n_e profiles change dramatically from peaked one to hollow with increase of the heating power. The value of n_e is non-zero at the last closed flux surface (LCFS), which is labeled as having a normalized radius ρ equal to 1, although T_e is almost zero at this position. This is due to the existence of an ergodic region, which is finite connection length and located outside of LCFS. The particle can be confined in this ergodic region. It is known from measurements of the spatial profile of H_α radiation that the peak of particle source is always located outside of LCFS surface when n_e at $\rho = 1$ is higher than $1 \times 10^{18} \text{m}^{-3}$. In addition, particle fuelling from NBI is negligible in these cases. Therefore, the distinction between n_e profiles in Fig.1 (b) is not due to the difference of the particle source deposition but due to the dissimilarity in the transport. The density profiles also vary with magnetic configuration. At similar collision frequencies, the n_e profiles tend to become hollower as R_{ax} increases [5]. In this paper, we concentrate only on the dependence of particle transport on heating power and B_t in standard configuration. The heating scheme used is NBI, whose power is scanned from 1MW to 8.5MW in this series of experiments. The line averaged density is almost kept constant to be free from the density dependence of the particle transport. Investigated plasmas lie in the plateau and so-called $1/\nu$ region, where helical ripple transport is enhanced. The normalized collisionality ($\nu^*_{h} = \nu_{ei} q R / \epsilon_{h,eff}^{1.5} \nu_{th}$) is 0.26~2.6 at $\rho=0.75$. The gas species is hydrogen.

3. Density Modulation Experiments in LHD

The particle flux can be written as the sum of diffusion and convection terms as follows:

$$\Gamma = -D\nabla n_e + n_e V . \quad (1)$$

The particle balance equation is the following:

$$\frac{\partial n_e}{\partial t} = -\nabla \cdot \Gamma + S = -\frac{1}{r} \frac{\partial}{\partial r} r \Gamma + S . \quad (2)$$

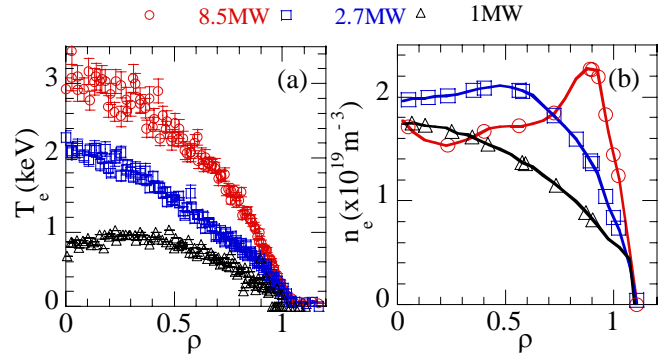


Fig.1 (a) T_e and (b) n_e profiles under different NBI heating power. At $R_{ax}=3.6\text{m}$, $B_t=2.75\text{T}$ for 2.7 MW and 8.5MW heating, $B_t=2.8\text{T}$ for 1MW heating. Temperature profiles are measured by Thomson scattering [1] and n_e profiles are measured by FIR [2] and CO_2 [3] laser interferometers.

Here, S is a particle source rate. If the particle source, which is located at the edge, is modulated, the density perturbation propagates from the edge to the core. The parameters D and V characterize this propagation. From the analysis of modulated components, D and V can be determined independently of the absolute value of the particle source [6], which is difficult to estimate experimentally. For this analysis, the source profiles (only relative shape) from 1-D calculations of the neutral penetration [7] are used.

Figures 2 (a) and (b) show the amplitude and phase profiles of line-integrated measurements for two discharges measured by the multi channel far infrared interferometer [2]. Modulation frequencies of 2, 5 and 10Hz are chosen to get several periods during the density flat top interval to ensure accurate measurements of phase and amplitude. A 5 Hz modulation was applied for the 5.2 MW heating case and 2 Hz modulation was applied for the 1 MW heating case. When core diffusion is lower, modulations cannot reach the core region and results become insensitive to core transport. Modulations at lower frequency can penetrate deeper in the core.

At lower heating power the diffusion is smaller as described in next section. So for the low diffusion case, a 2 Hz modulation was employed to estimate core diffusion coefficients. The modulation amplitude is kept less than 4 % of line averaged density in order that the underlying transport is not modified.

The modulated part of particle balance equation can be expressed in cylindrical geometry by the following equation:

$$\frac{\partial^2 \tilde{n}_e}{\partial r^2} + \left(\frac{1}{r} + \frac{1}{D} \frac{\partial D}{\partial r} - \frac{V}{D} \right) \frac{\partial \tilde{n}_e}{\partial r} - \left(\frac{V}{rD} + \frac{1}{D} \frac{\partial V}{\partial r} \right) \tilde{n}_e - i \frac{\omega}{D} \tilde{n}_e + \frac{\tilde{S}}{D} = 0. \quad (3)$$

Here, tilde symbols indicate modulated components; ω indicates modulation frequency. The n_e tilde is complex function, which has amplitude and phase information. The D and V are obtained from the fitting the solution of Eq. (3) to experimental data. Since the interferometer measures line integrated quantities, line-integrals of solutions to Eq. (3), parameterized by D and V , are fitted to the measured data.

Figures 2 show examples of integrated modulation amplitude and

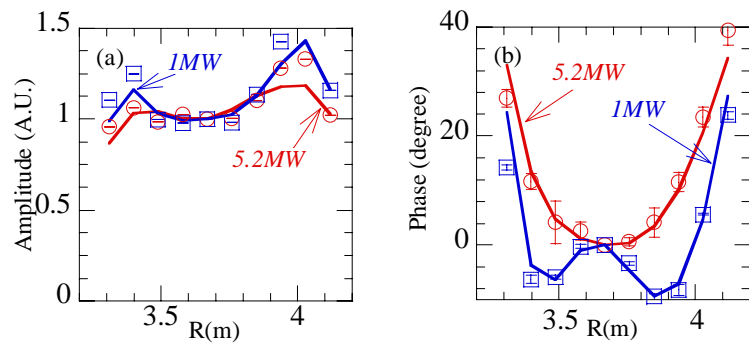


Fig.2 Comparison of modulation amplitude (a) and phase (b) profiles at different heating power. Circular and square symbols indicate measured values, lines indicate calculated values.

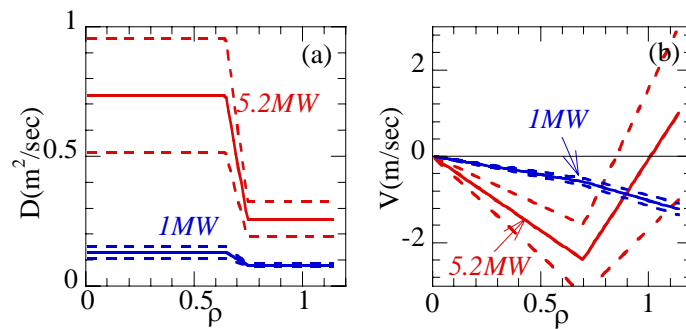


Fig.3 Estimated (a) D and (b) V . The dashed lines indicate upper and lower error. The positive and negative V indicates outward and inward convection.

phase at different heating power. A clear difference is observed between two cases. The amplitude and phase are calculated by the correlation analysis. The error bar is the uncertainty of the determination of phase and amplitude. The amplitude and phase profiles are calculated using model profiles of D and V as shown in Fig.3. Because the core and edge transport can be different, two fitting variables for both D and V are used. One is the core value ($D_{\text{core}}, V_{\text{core}}$) and the other is edge value ($D_{\text{edge}}, V_{\text{edge}}$). The D are assumed to be constant in the core and edge and change at $\rho = 0.7$. The value of V is zero at $\rho = 0$ and V profiles are assumed to vary linearly with ρ , changing slope at $\rho = 0.7$. The values of V at $\rho = 0.7$ and $\rho = 1.0$ are taken to represent V_{core} and V_{edge} respectively. The transition points of D and V are fixed at $\rho = 0.7$ in this series of analysis in order to make fitting more stable. As shown in Fig.2, measurements and calculation agree reasonably. The estimation errors of D and V in Fig.3 originate from estimation inaccuracy of modulation amplitude and phase.

4. Characteristics of transport coefficients

4.1 Particle Diffusion

As shown in Fig. 3 (a), the D is higher in the core and edge for both cases. Figure 4 shows the profile of electron thermal diffusion coefficients χ_e obtained from power balance analysis by using PROCTR [7] code. Typically, the χ_e profiles also show larger values in the core as well in LHD at standard configuration [5]. The predominance of core value of D and χ_e was also observed in this series of modulation experiments. The lower values of D and χ_e in the edge region are the reason for the steep edge gradients of n_e and T_e , which is observed in Fig.1 (a) and (b). The strong magnetic shear may play a role to stabilize micro instabilities and reduce diffusion in the edge region. The value of χ_e is around one order magnitude larger than D . This is similar to the case of typical tokamak experiments.

A comparison of the experimentally determined D with a neoclassical estimate, calculated by the DCOM [9] code is presented in Fig. 5. In both cases, the experimental value is one order of magnitude larger than the neoclassical estimate. The diffusive particle flux is predominantly anomalous. This suggests that micro turbulence plays an important role on diffusive flux.

The temperature dependence of D forms the basis for the investigation of the anomalous transport model. For Bohm-like diffusion, where particle transport is influenced by the long-wavelength fluctuations (up to plasma minor radius), D is proportional to T_e , while for gyro-Bohm-like diffusion, where short-wavelength fluctuations (around the ion gyro-radius) play a role, D is proportional to $T_e^{1.5}$. For this investigation, a systematic scan of NBI heating power ($P = 1 \sim 8.5 \text{ MW}$) keeping background density almost constant ($n_{e\text{-bar}} = 1.2 \sim 1.5 \times 10^{19} \text{ m}^{-3}$) is carried out at $R_{\text{ax}} = 3.6 \text{ m}$. The data set contains discharges at $B_t = 2.8$ and 2.75 T . The

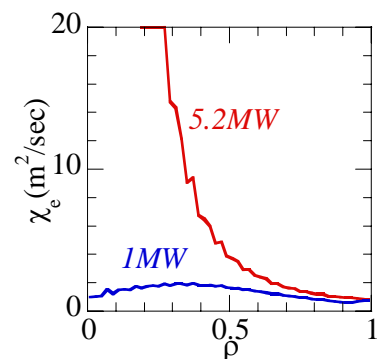


Fig.4 χ_e profiles from power balance analysis

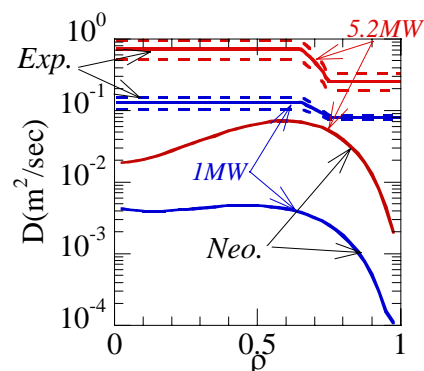


Fig.5 Comparison with neoclassical estimation

small difference of B_t is not expected to affect the transport.

Figure 6 shows the T_e dependence of D_{core} and D_{edge} . The electron temperature in Fig.6 is the averaged value within $\rho = 0.4 \sim 0.7$ for the core and $\rho = 0.7 \sim 1.0$ for the edge. The data set include 2, 5, and 10Hz modulation frequencies. When core diffusion coefficients cannot be determined from fitting because of lower diffusion or higher modulation frequency, a spatially constant profile is assumed. Then estimated D was used as a D_{edge} , because the analysis has sensitivity in the edge region in this case. The diffusion coefficient increases with T_e both in the core and edge regions. The fitted power-law scaling of the observed T_e dependences are $D_{\text{core}} \propto T_e^{1.7 \pm 0.9}$ and $D_{\text{edge}} \propto T_e^{1.1 \pm 0.14}$. The difference of the T_e

dependence in the core and edge suggests the existence of different types of turbulence in the core and edge. From the T_e dependence, D_{core} is gyro Bohm like rather than Bohm like. However, for the edge region the distinction between the two models is not so clear.

4. 2 Particle Convection

Hollow density profiles are observed in LHD in many discharges. This is a harsh contrast to tokamak plasmas, where most density profiles are peaked. As is shown in Fig.1, n_e profiles become hollow with an increase of T_e . The hollow density profiles clearly indicate the existence of the outward convection, because the particle source, which is localized out of LCFS, cannot maintain the hollow density profiles. In addition, density modulation experiments can estimate D and V separately, and results of many experimental discharges show an existence of the particle convection, which is the second term of Eq.(1). This fact suggests that off-diagonal terms of transport matrix contribute to the total particle flux. For example, to sustain the positive density gradient, which is observed at $\rho = 0.6 \sim 0.9$ in 8.5MW heating case (see Fig.1(b)), in the equilibrium state, off-diagonal transport coefficients should determine the particle flux, since diffusion does not contribute to total particle flux in this region. The next question is which driving term or which gradient determines convective flux.

The change of the n_e profile in Fig.1 (b) suggests a correlation between V and T_e gradients (∇T_e). Figure 7 shows the T_e gradient dependence of V . The value of V at $\rho = 0.7$ is considered to be V_{core} , and V_{edge} is considered to be the value at $\rho = 1.0$. The electron temperature gradient is the averaged over the region $\rho = 0.4 \sim 0.7$ for core and $\rho = 0.7 \sim 1.0$ for the edge. The edge convection is inward directed in the most of the case. On the other hands, V_{core} changes direction from inward to outward with increasing of T_e gradient. The temperature gradient dependence of V_{edge} is not very clear although there is a modest tendency of decreasing V_{edge} with increasing ∇T_e . The dependence of V_{core} on ∇T_e is more pronounced. The core convection velocity shows a clear dependence on ∇T_e . Comparison

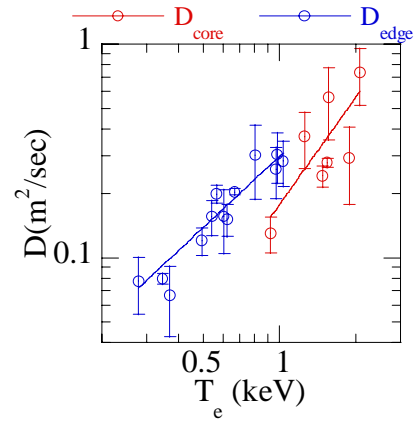


Fig. 6 T_e dependence of D at $R_{ax}=3.6m, B_t=2.75, 2.8T$.

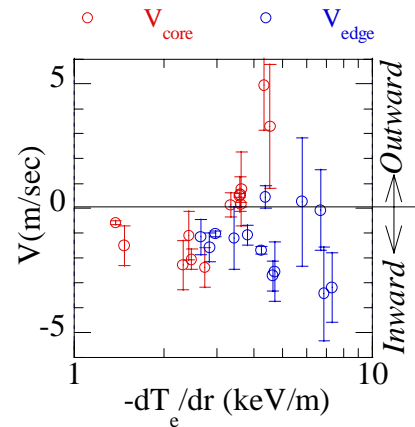


Fig.7 $\text{Grad } T_e$ dependence of V

with theoretical model for turbulence [10] is necessary for further understanding of the convection term.

4.3 The Effects of the Toroidal Magnetic Fields

The effect of B_t can give more clear remarks about whether diffusion is Bohm like (D is proportional to B^{-1}) or gyro-Bohm like (D is proportional to B^{-2}). The modulation experiments were done to study the effect of B_t on D and V . A comparison is made between two discharges at different B_t (1.49 and 2.75 T). In order to be free from the n_e and T_e dependence of D and V , the heating power and gas fuelling were adjusted to produce almost identical T_e profiles and similar line averaged density.

A results for the estimated D and V are summarized in table.1. Since a relatively high modulation frequency of 10Hz was used to make the analysis possible during the short density flat top (~ 1 sec), a constant D profile, which mostly represents the edge value, is used for this analysis.

At $B_t = 1.49$ T, a strongly hollow profile was observed and corresponding to this, the estimated V_{core} is outward directed. On the other hand, at $B_t = 2.75$ T, flat density profiles are observed and the convection was observed to be inward directed in both the core and edge. Compared with the results of 4.2, which show a clear relationship between V_{core} and ∇T_e , it seems that the magnetic field also plays a significant role. One possible explanation is that the critical temperature gradient which reverses the direction of V_{core} is the function of B_t . The other possibility is the existence of other convection driving terms in addition to ∇T_e . More detailed investigations of the ∇T_e dependence at different B_t are required to conclude this question.

The B_t dependence of D , which represent edge value is $B_t^{-2.08}$, which is very close to gyro-Bohm diffusion. Considering the T_e dependence ($D_{\text{edge}} \propto T_e^{1.1 \pm 0.14}$), the edge diffusion is gyro-Bohm like rather than Bohm like. The gyro-Bohm nature is same as thermal diffusivity [4].

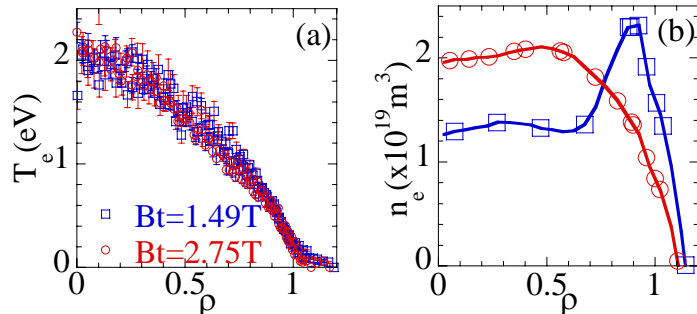


Fig. 8 Comparison of (a) T_e and (b) n_e profiles under different B_t .

TABLE I: Effect of B_t on D and V

Shot	B_t (T)	D_{edge} (m ² /sec)	V_{core} (m/sec)	V_{edge} (m/sec)
48619	1.49	0.43 ± 0.13	5.43 ± 2.89	-2.67 ± 2.87
48672	2.75	0.12 ± 0.004	-2.59 ± 0.45	-3.32 ± 0.28

5. Characteristics of Turbulence

As shown in Fig.5, diffusion is dominated by anomalous terms. To get a comprehensive picture of particle transport, it is absolutely essential to measure micro turbulence. The spatial spectrum structure of fluctuations, dependence on the parameters of the discharge and correlation with transport characteristics can provide ideas to understand

anomalous transport. In LHD, micro turbulence was measured by using a CO₂ laser Phase Contrast Imaging (PCI) Interferometer [11,12,13]. Since the length of scattering volume for the expected wavenumber region is larger than the plasma size for the 10.6 μ m infrared CO₂ laser wavelength, no spatial resolution is expected along beam axis. However, by using strong magnetic shear of LHD, it is possible to get modest spatial resolution along the probe beam [14].

The qualitative difference of the fluctuation spectra is observed at different NBI heating powers using PCI. Figure 9 shows wavenumber (k) and frequency (f) spectra, which are measured by PCI at different heating power and similar line averaged density. Spatial resolution is around the minor radius, and the range of wavenumber is $k = 0.1 \sim 1.25 \text{ mm}^{-1}$. The measured wavenumber is comprised mostly of poloidal components. The observed frequency range is 5~125 kHz. The peak wavenumber is 0.2 mm^{-1} at 1MW heating and 0.3 mm^{-1} at 6.5 MW heating. The value of $k_{\perp} \rho_i$ is around 0.1, which is roughly equal to that expected for the gyro-Bohm diffusion model. In both cases, fluctuations propagate in the electron diamagnetic direction in the laboratory frame at around the drift velocity. It is necessary to exclude the Doppler shift at the $E_r \times B_t$ rotation velocity, however, measurements of E_r were not available in these shots.

As observed in Section 4.1, higher heating power causes larger diffusion. This observation can be compared with the properties of the fluctuations. As the diffusion coefficient is proportional to $(\text{step size})^2 / (\text{step time})$, the anomalous component can be expressed as the $(\text{fluctuation wavelength})^2 / (\text{growth rate of fluctuation}) \sim (\text{frequency width}) / (\text{wave number})^2$. As shown in Fig.9, broad spectra in k it is observed that the value of k at the peak of the wavenumber spectrum is reduced and the frequency spectrum is broadened at higher heating power. This is qualitatively consistent with enhanced diffusion at higher heating power. The shifting of peak wavenumber to lower values, when energy confinements degrade at lower B_t , is also observed in LHD [11].

Recently, a new technique was developed to measure spatial profile of fluctuation [12, 13]. By using 48 (6 by 8) channel two dimensional detector, it is possible to get fluctuation

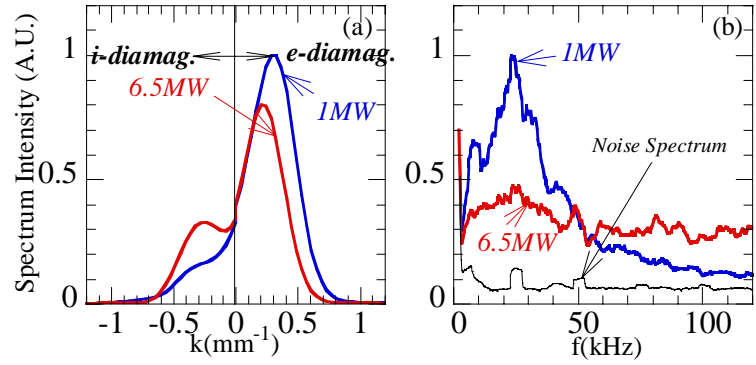


Fig.9 Comparison of (a) k and (b) f spectrum under different heating power. $R_{ax}=3.6m$. $B_t=2.8T$

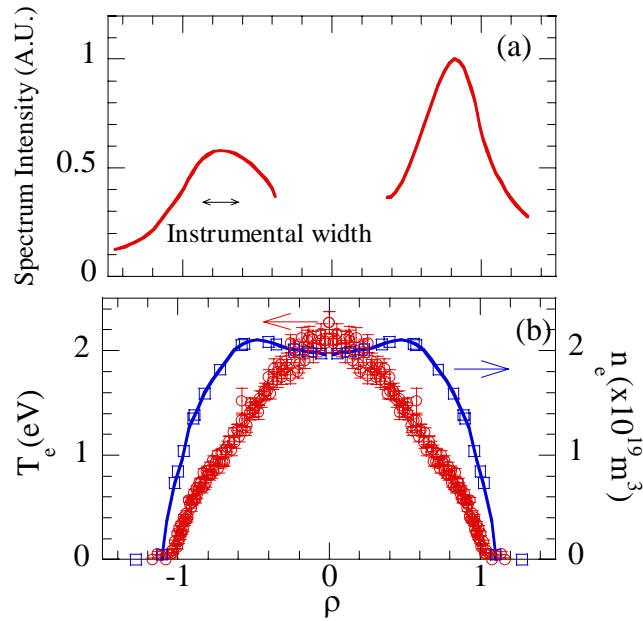


Fig.10 (a) Spatial profile of fluctuation ($0.5 < k < 1.5 \text{ mm}^{-1}$) and (b) n_e , T_e profile. $R_{ax} = 3.6m$, $B_t = 2.75T$

profile from single shot and single time by taking advantage of the strong magnetic shear. The spatial resolution is around one fifth of minor radius for $k = 0.5 \sim 1.5 \text{ mm}^{-1}$. Figure 10(a) shows a spatial profile of the fluctuation power. Positive and negative ρ indicate the upper and lower parts of the vertical elongated cross section respectively. The fluctuation peaks are localized in edge region. As shown in Fig. 5, D_{core} is larger than D_{edge} , however, since the density gradient tends to be flat in the core as shown in Fig.1(a) and Fig.10(b), diffusion does not contribute to the total particle flux in the core in the equilibrium state. On the other hand, diffusion contributes more than convection in the edge region, where the negative density gradient is steep. In addition, the D_{edge} is one order of magnitude larger than the neoclassical estimate as shown in Fig. 5. Therefore, the observed fluctuations localized in the edge region can contribute diffusive particle flux. From present dataset, however, the role of fluctuations on convection is not clear.

6. Summary

Systematic studies by using density modulation experiments were done to investigate particle transport characteristics at standard magnetic configuration in LHD. The density profiles vary with heating power and B_t . The edge diffusion coefficient is close to gyro-Bohm nature, where fluctuation wavelength around ion Larmor radius play an important role. The diffusion coefficient is larger in the core than at the edge. Strong particle convection is observed. The core convection velocity shows clear dependence on the T_e gradient. As the T_e gradient is increased, V_{core} changes direction from inward to outward. This is consistent with the fact that the density profile changes from peaked to hollow with an increase of heating power. However, B_t is also a key parameter to determine V_{core} . The edge convection velocity is inward directed in the most cases. A moderate tendency to decrease V_{edge} with increasing T_e gradient is also observed. The micro turbulence measured by PCI shows qualitative correlation with particle diffusion. More detailed systematic study about the density dependence and effect of magnetic configuration are underway and comparison with theoretical models of transport and turbulence is planned.

References

- [1] K. Narihara et al., Rev. Sci. Instrum., 72 (2001) 1122.
- [2] K. Kawahata et al., Rev. Sci. Instrum. **70**, (1999) 707.
- [3] K. Tanaka et al., to be published Rev. Sci. Instrum.
- [4] H. Yamada et al., in 18th Conference Proceedings of Fusion Energy 2000 (Sorrento, Italy 4-10 October 2000) IAEA (2001).
- [5] K. Tanaka et al., J. Plasma Fusion Res. Series, 4 (2001) 427.
- [6] K.W. Gentle et al., Plasma Phys. Contr. Fusion 29, (1987) 1077.
- [7] H.C. Howe, ORNL/TM-11521 (1990).
- [8] H. Yamada et al., Plasma Phys. Contrl. Fusion 44 (2002) A245.
- [9] S. Murakami et al., Nuclear Fusion 42 (2002) L19-L22.
- [10] X. Garbet et al., Phys. Rev. Lett. 91 (2003) 035001-1.
- [11] K. Tanaka et al., Rev. Sci. Instrum., Vol 74 (2003) pp1633-1637.
- [12] A. Sanin et al., to be published Rev. Sci. Instrum.
- [13] L. N. Vyacheslavov et al., to be published 4th Triennial Special Issue of IEEE Transaction on Plasma Science.
- [14] S. Kado et al, Jpn. J. Appl. Phys., Part 1 34, (1995) 6492.